

## Corrosion-Resistant Epoxy Coatings Filled with Nanoparticles of Vegetable Origin to Protect Water Vehicles

O.O. Sapronov<sup>1</sup>, K. Dyadyura<sup>2</sup>, P.O. Vorobiov<sup>1</sup>, V.D. Sharanov<sup>3</sup>, M.O Karpash<sup>4</sup>, R.T. Bishchak<sup>5</sup>,  
L. Hrebenyk<sup>6</sup>

<sup>1</sup> Kherson State Maritime Academy, Kherson, Ukraine

<sup>2</sup> Odesa Polytechnic National University, 1, Shevchenka Ave, 65044 Odesa, Odessa Oblast, Ukraine

<sup>3</sup> Danube Institute of the National University "Odesa Maritime Academy", Izmail, Ukraine

<sup>4</sup> King Danylo University, Ivano-Frankivsk, Ukraine

<sup>5</sup> Ivano-Frankivsk National Technical University of Oil and Gas, Ivano-Frankivsk, Ukraine

<sup>6</sup> Sumy State University Medical Institute, 28, Troytska Str., 40022 Sumy, Ukraine

(Received 05 August 2023; revised manuscript received 18 October 2023; published online 30 October 2023)

The structure of the developed epoxy coatings using IR spectral analysis and corrosion resistance by determining the permeability index in the aggressive environment of river water during  $t = 6552 h$  at a temperature range  $T = 258...303 \pm 2 K$  was investigated in the article. It was shown that the process of structure formation of epoxy coatings is influenced by the change in the ratio of nano-disperse and fibrous fillers in epoxy ED-20 oligomer. Significant structural changes for epoxy coatings were observed at wave numbers:  $\nu = 570 cm^{-1}$ ,  $\nu = 840 cm^{-1}$ ,  $\nu = 1045 cm^{-1}$ ,  $\nu = 2962 cm^{-1}$ , which indicates their degree of crosslinking. A study on the change in the permeability index in the environment of river water was carried out with consideration of rational proportion of dispersive fillers in the epoxy binder, which made it possible to create an effective barrier to the penetration of aggressive ions and water molecules to the base. A decrease in the permeability of protective coatings by 1.8 ... 2.0 times relative to the epoxy matrix was achieved. In addition, a visual analysis of the surface coatings operated under the influence of river water at variable temperatures was carried out. For the epoxy matrix and composites containing one filler, defects in the form of cracks and peeling were observed, which are associated with the course of physical and chemical processes of sorption and diffusion of an aggressive environment. In addition, such coatings are characterized by a tendency to overgrowth with green algae of the genus Spirogyra. For the coatings containing a rational combination of two fillers, the absence of defects and biological fouling was observed.

**Keywords:** Epoxy binder, Filler, Defect analysis, IR Spectral analysis, Permeability index, Corrosion, Nanopowder.

DOI: [10.21272/jnep.15\(5\).05025](https://doi.org/10.21272/jnep.15(5).05025)

PACS numbers: 81.05.t, 81.05.Zx

### 1. INTRODUCTION

Corrosive destruction of underwater and surface parts of ship hulls, fittings, pipeline systems, hulls of units for various purposes, and metal structures with permanent contact with water significantly reduces their service life, leading to additional economic costs associated with their operation, maintenance, and repair. Therefore, improvement of functional characteristics of water transport is possible through the use of modified polymer [1, 2] coatings, which allows to counteract the corrosion destruction of metal surfaces and equipment and metal films as protective layers [3, 4]. At the same time, inhibitors or inhibitory pigments are used to modify the polymer binder. The use of anti-corrosion pigments in the system of organic coatings is an effective protection against corrosion [5, 6]. One of the inhibitory pigments is chromates, which have high anti-corrosion performance, allow operation in a wide pH range of the environment, and are cost-effective [7]. Thus, the authors of the work [6-8] showed that the use of chromates in the way of microencapsulation is one of the promising approaches that ensure the effective protective effect of polymer coatings. A microcapsule contains a shell and a core, which can provide different functions. In this case, the microcapsule provides inhibitory and restorative effects. That is, in the event

of mechanical damage, the microcapsule shell ruptures, as a result of which active substances are released and fill the crack, as a result of which the substrate is protected. The authors of the paper [9] synthesized polyurea-based microcapsules containing a quinoline corrosion inhibitor dispersed in a polyurethane coating. It was demonstrated that adding 4 wt. % of microcapsules leads to an increase in corrosion resistance. It was shown [10] that the use of microcapsules based on urea-formaldehyde, linseed oil, cerium acetate (Ce) (corrosion inhibitor), and 8-hydroxyquinoline (8-HQ) (corrosion inhibitor and indicator) provides a significant inhibitory effect of polymer protective coatings. Protective coatings filled with microcapsules based on urea-formaldehyde and a mixture of 50 wt. % Ce and 50 wt. % 8-HQ provides detection of the corrosion process using the fluorescence mechanism, as well as its inhibition. Among the existing pigments, phosphate-containing pigments are belonging to the electrochemical active class [11, 12]. Zinc phosphate (ZP) pigment is often used in organic coatings to replace chromium-based pigments, which are toxic despite a significant protective effect [13, 14]. However, zinc phosphate is a scarce material compared to chromate [15, 16]. At the same time, it has been proven [17-19] that the use of nitrites can prevent the pitting corrosion of steel. Compared to other heavy metal corrosion ions-

inhibitors, such as  $(\text{CrO}_4^{2-}, \text{WO}_4^{2-}, \text{MoO}_4^{2-}, \text{Cr}_2\text{O}_7^{2-})$ , nitrites have less negative environmental impact. Cao et al. [20, 21] showed that the use of  $\text{NO}_2^-$  inhibitor provides effective corrosion control of carbon steel in aggressive environments.

However, it should be noted that today there are certain restrictions for the use of anti-corrosion paints for water transport containing metal biocides, in particular polymer systems based on tributyltin, copper, and zinc [22]. In addition, EU and US regulatory acts limit the use of chromates, phosphates, and nitrites, which makes it difficult for businesses to produce chromate-containing and phosphate-containing paints and varnish materials. Therefore, today considerable attention is paid to the selection and research of environmentally safe components of polymer coatings intended for corrosion protection of water transport. At the same time, one of the ecological ("green") alternatives that can replace the above traditional additives is the use of fillers of natural origin.

The work aims to investigate the influence of the content of dispersed additives on the degree of crosslinking and corrosion resistance of the developed epoxy coatings.

## 2. MATERIALS AND METHODS

### 2.1 Research Materials

As the main component for the binder in the formation of epoxy composite materials (CMs), ED-20 epoxy dian oligomer (ISO 18280:2010, Technobudresurs, Kyiv, Ukraine) was chosen, which is characterized by high adhesive and cohesive strength, slight shrinkage and manufacturability when applied to the surface of a complex profile. For cross-linking of the epoxy binder, cold hardening hardener polyethylene polyamine (PEPA) was used.

An additive of vegetable origin was used as a filler for experimental studies. The primary form of the additive is pressed briquettes based on secondary products of plant processing with the size:  $d = 60$  mm,  $l = 80 - 150$  mm. Ash content is 2.8 %, density at  $0.855$  g/cm<sup>3</sup>. The final product is a filler with a size of  $400 \dots 600$  nm, which is obtained as a result of the thermal decomposition of pressed organic material.

In addition, a mixture of discrete fibers based on cotton and polyester was used: MFCP (cotton – 52 %, polyester – 48 %) with parameters  $l = 15 \dots 30$  mm,  $d = 20 \dots 25$  μm.

The technology of CM forming was carried out in a certain sequence, which is described in scientific works [1, 26-30]. The following properties of CM were studied in the work: structure and corrosion resistance of the developed coatings.

### 2.2 Research Methodology

The IR spectroscopy method was used to study the structure of polymer coatings. IR spectra were deciphered according to the methodology outlined in the works [26, 27]. IR spectra were recorded on an IRAffinity-1 spectrophotometer (Japan) in the range of

wave numbers  $\nu = 400 \dots 4000$  cm<sup>-1</sup> by the single-beam method in reflected light. Spectrum sweep by wave numbers  $\lambda^{-1} = \nu$  was done on the diagram within 225 mm in the range of selected frequencies. Wave numbers, transmission intensity, and absorption band area were determined using the IRsolution software. The error in determining the wave number was  $\nu = \pm 0.01$  cm<sup>-1</sup>, while in determining the accuracy of the peak location, it was  $\nu = \pm 0.125$  cm<sup>-1</sup>. The photometric accuracy was  $\pm 0.2$  % with software control of the slit and the duration of integration  $t = 10$  s. The integration step is  $\Delta\lambda = 4$  cm<sup>-1</sup>.

The corrosion resistance of protective coatings was determined by immersing the samples in river water (Hydrobiological Station, Kherson). The duration of exposure of samples with dimensions of  $90.0 \times 90.0 \times 2.0$  mm in the aggressive environment of river water was  $t = 6552$  h (9 months) at a temperature of  $T = 258 \dots 303 \pm 2$  K (within the period from 01.11.21 to 01.07.2022). A coating with a thickness of  $h = 718 \dots 815$  μm was applied to structural steel samples - Steel 2 by a mechanical method, while the coverage area was  $S = 81.0$  cm<sup>2</sup>.

Coated samples weighing  $91.3 \dots 96.0 \pm 0.2$  g before experiments and after exposure to aggressive environments were weighed at electronic balance DRS-8000 "Shimadzu" with an accuracy of  $0.02 \pm 0.001$  g.

If the weight of the samples increases, the permeability index of the aggressive environment is calculated according to the formula [2]:

$$\chi = \frac{b-a}{a} \cdot 100\%, \quad (2.1)$$

and if the weight of the samples is reduced, the permeability index of the aggressive environment is calculated according to the formula [2]:

$$\chi = \frac{a-b}{a} \cdot 100\%, \quad (2.2)$$

where:  $\chi$  – corrosion resistance, %;  $a$  – mass of samples to be tested, g;  $b$  is the mass of the samples after the exposure, g.

The deviation of the mass values during corrosion resistance studies of the developed CM was  $4 \dots 6$  % from the nominal value.

In addition, a visual analysis of the coatings was performed under the above-mentioned conditions and the influence of an aggressive environment. Defects of protective coatings were studied, in particular edge corrosion, cracking, peeling, and biological fouling.

## 3. DISCUSSION OF RESEARCH RESULTS

Based on the preliminary results of the mathematical planning of the experiment, the composition of CM was selected, the structure of which was studied by the method of IR spectral analysis, to determine the degree of crosslinking of the developed coatings. IR spectral analysis of the epoxy matrix and filled composites with a mixture of various additives of vegetable origin was carried out, namely (Fig. 1):

– matrix (control sample): the matrix was formed

using the following ratio of components ( $q$ , wt. parts) – epoxy oligomer ED-20: hardener PEPA – 100:10;

– CM 1 (the composite formed according to the following ratio of components ( $q$ , parts by mass) - binder: a mixture of discrete fibers based on cotton and polyester (MFCP) ( $l = 15 \dots 30$  mm,  $d = 20 \dots 25$   $\mu\text{m}$ ): nanofiller of vegetable origin (NVO) ( $d = 400 \dots 600$  nm): hardener – 100: 0.25: 0.075: 10);

– CM 2 (the composite formed according to the following ratio of components ( $q$ , parts by mass) - binder: a mixture of discrete fibers based on cotton and polyester (MFCP) ( $l = 15 \dots 30$  mm,  $d = 20 \dots 25$   $\mu\text{m}$ ): nanofiller of vegetable origin (NVO) ( $d = 400 \dots 600$  nm): hardener - 100: 0.25: 0.100: 10);

– CM 3 (the composite formed according to the following ratio of components ( $q$ , parts by mass) - binder: a mixture of discrete fibers based on cotton and polyester (MFCP) ( $l = 15 \dots 30$  mm,  $d = 20 \dots 25$   $\mu\text{m}$ ): nanofiller of vegetable origin (NVO) ( $d = 400 \dots 600$  nm): hardener - 100: 0.50: 0.075: 10);

– CM 4 (the composite formed according to the following ratio of components ( $q$ , parts by mass) - binder: a mixture of discrete fibers based on cotton and polyester (MFCP) ( $l = 15 \dots 30$  mm,  $d = 20 \dots 25$   $\mu\text{m}$ ): nanofiller of vegetable origin (NVO) ( $d = 400 \dots 600$  nm): hardener – 100: 0.50: 0.100: 10).

The change in the number of bonds – C – C – in epoxy composites ( $\nu = 570$   $\text{cm}^{-1}$ ) was determined by the method of IR spectral analysis. It was shown that CM3 is characterized by the maximum peak area of  $S = 69.8$  %, which indicates an increase in the number of cross-links, and, therefore, an increase in the strength of the polymer mesh frame. Then, as for CM 1, CM 2, and CM 4, a decrease in the number of – C – C – bonds was observed. A different ratio of components (MFCP: NVO) in the epoxy binder affects the strength indicators of the polymer. Additionally, it was found out that the change in intensity and peak area at  $\nu = 769$   $\text{cm}^{-1}$  characterizes the displacement of hydrogen atoms in methyl groups relative to carbon atoms in the direction of the C–H bond, which may indirectly indicate the elastic characteristics of the composite. An increase in the intensity and relative area of the peaks at  $\nu = 840$   $\text{cm}^{-1}$  for CM 3 and CM4 indicates an increase in – C – C – bonds and amine groups in the polymer structure. At the same time, an increase in the intensity and relative area of the peaks at  $\nu = 1045$   $\text{cm}^{-1}$  was observed for CM 3 and CM 4, which indicates an increase in C–O–C epoxy groups in the polymer structure. It was supposed that this is due to the reactive interaction of the epoxy oligomer with active amines and carboxyl groups, which are present in supplements of vegetable origin. At  $\nu = 1892$   $\text{cm}^{-1}$ , a signal corresponding to carbonyl groups located close to C – O – C epoxy groups was obtained, while significant changes in the intensity and relative area of the peaks were not found. Similarly, stable values of the intensity and relative peak area at  $\nu = 2067$   $\text{cm}^{-1}$  and  $\nu = 3439$   $\text{cm}^{-1}$  were established for the composites under study.

The analysis of IR spectra at  $\nu = 2962$   $\text{cm}^{-1}$  allows us to state an increase in the number of asymmetric and symmetric vibrations of C – H bonds in the methyl and methylene groups of the crosslinked polymer (CM2, CM3, CM4), which indicates the presence of a

greater number of CH and CH<sub>3</sub> groups in the polymer structure. This, in turn, can be an indicator of increased hydrophobicity and resistance to oxidation and other chemical reactions, since C – H bonds in methyl and methylene groups refer to carbon bonds with relatively high strength. Therefore, an increase in the number of such bonds provides an improvement in the mechanical and chemical properties of polymers.

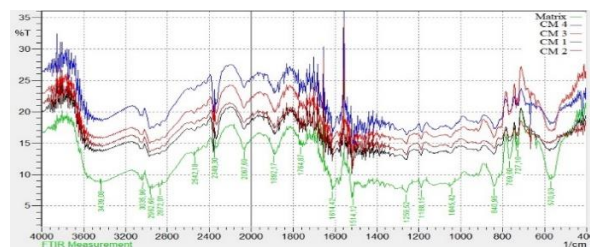


**Fig. 1** – IR spectra of composites in the range of wave numbers  $\nu = 400 \dots 4000$   $\text{cm}^{-1}$ : 1 – epoxy matrix; 2 – CM 1 (MFCP: NVO – 0.25 : 0.075); 3 – CM 2 (MFCP: NVO – 0.25 : 0.100); 4 – CM 4 (MFCP: NVO – 0.50 : 0.075); 5 – CM 3 (MFCP: NVO – 0.50 : 0.100)

Based on IR spectral analysis, the existence of a wide spectrum of peaks that characterize the fluctuations of side groups and segments of polymer macromolecules was established. It should be noted that the given IR spectra have a similar character (Fig. 1). However, after adding the additives that contain components of vegetable origin a change in peak parameters was observed (Table 1), namely, the transmission intensity ( $T$ , %) and the relative peak area ( $S$ , %) changed.

This indicates on a different number of chemical bonds in the polymer, and, therefore, a change in the degree of crosslinking of the developed composites [26, 29]. Based on the analysis of IR spectra, an increased degree of crosslinking of the composites was established:

– CM 3, which contains in its composition – a binder: a mixture of discrete fibers based on cotton: a nanofiller of vegetable origin: and a hardener – in the ratio ( $q$ , wt.): 100: 0.50: 0.075 : 10;

– CM 4, which contains in its composition – a binder: a mixture of discrete fibers based on cotton: a nanofiller of vegetable origin: and a hardener – in the ratio ( $q$ , wt.): 100: 0.50: 0.100: 10.

Further, the materials CM 3 and CM 4 were tested under conditions of exposure to the aggressive environment of river water at variable temperatures for corrosion resistance. At the same time, the epoxy matrix and two coatings (CM 1, CM 2) containing only one filler, the optimal content of which was established in previous works, were additionally tested, namely:

– matrix (reference sample) was formed using the following ratio of components ( $q$ , wt.) – epoxy oligomer ED-20: hardener PEPA – 100: 10;

– CM 1 was formed using the following ratio of components ( $q$ , wt.) – binder: nanofiller of vegetable origin (NVO) ( $d = 400 \dots 600$  nm): hardener – 100: 0.100 : 10;

– CM 2 was formed according to the following ratio of components ( $q$ , wt.) – binder: a mixture of discrete fibers based on cotton and polyester (MFCP) ( $l = 15 \dots 30$  mm,

$d = 20 \dots 25 \mu\text{m}$ ): hardener – 100 : 0.50 : 10.

Before applying the protective coatings, the metal base was mechanically cleaned (Fig. 2, a-e), to remove rust and other contaminants, as well as to degrease the metal surface using acetone ( $\text{C}_3\text{H}_6\text{O}$ ). The coating was applied to metal plates made of structural steel – St 2, size  $90 \times 90 \times 2.0 \text{ mm}$  on one side.

**Table 1** – Characteristic absorption bands according to IR spectral analysis of the original matrix and filled epoxy composites

Band features		IR spectra of initial epoxy matrix and composites									
		Initial matrix		CM 1		CM 2		CM 3		CM 4	
Group	$\nu, \text{cm}^{-1}$	T, %	S, %	T, %	S, %	T, %	S, %	T, %	S, %	T, %	S, %
-C-C- valence oscillations	570	9.3	63.4	14.0	40.3	15.1	38.2	17.3	69.8	18.3	44.6
Fluctuations of C-H valence bonds in methyl groups – $\text{CH}_3$	769	12.4	25.2	15.1	19.1	15.7	18.2	20.1	25.9	19.7	21.3
-C-C- valence oscillations, amino groups: $\text{CH}_2\text{-NH}_2$ , $\text{CH-NH}_2$	840	8.1	39.2	13.8	32.3	14.2	32.1	17.0	38.3	16.1	33.4
Oscillations of epoxy groups C-O-C	1045	8.2	15.3	13.6	16.1	14.0	16.8	17.2	17.3	16.0	18.2
Carbonyl group C=O	1892	13.3	64.3	16.9	64.1	17.2	64.2	23.0	64.3	21.0	64.3
-C $\equiv$ N- valence oscillations	2067	13.9	65.4	17.5	65.2	18.2	65.2	24.0	65.4	20.8	65.4
Asymmetric and symmetric oscillations of C-H bonds in methyl and methylene groups	2962	7.8	50.1	13.2	51.2	14.6	51.6	17.8	52.8	15.1	51.6

-OH - valence vibrations, vibrations of -HH bonds of amino groups											
	3439	8.8	97.1	13.6	97.3	14.8	97.3	18.5	98.5	16.0	98.5

For a visual examination of defects formed on the surface, T-shaped cuts were made on the formed coatings (Fig. 2). Before immersion to a depth of 2.0 – 2.5 meters into the river water applied coating onto the metal base was weighed using electronic scales DRS-8000 "Shimadzu". Thickness was measured using an electronic thickness gauge CM8811FN with an error of  $\pm 2 \mu\text{m}$  (Table 2). Based on the obtained values of the weight of the samples before and after the exposure the permeability index of the aggressive environment was determined, which made it possible to determine the corrosion resistance of the developed protective coatings.

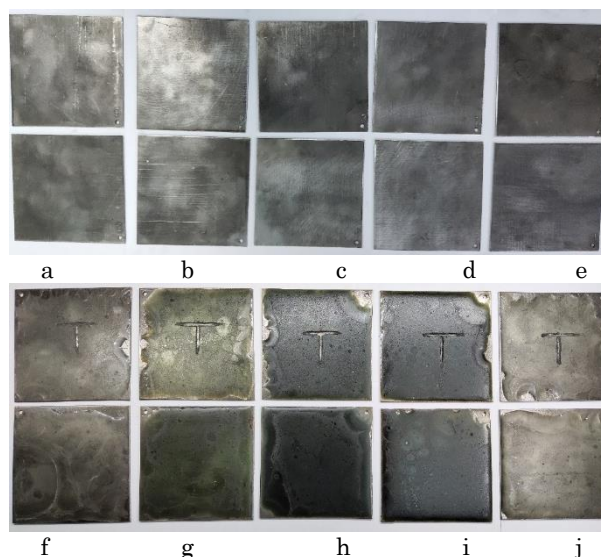


**Fig. 2** – General view of applied coatings: a-e – base; f – CM 1; g – CM 2; h – CM 3; i – CM 4; j – epoxy matrix

The change in the permeability index and the nature of surface defects of epoxy composite coatings without T-shaped cuts were previously inspected.

It was shown (Table 2) that the epoxy matrix is characterized by the highest value of the permeability index  $\chi = 1.90 \%$  in the environment of river water. It was supposed that the influence of variable temperatures  $T = 258 \dots 303 \pm 2 \text{ K}$  during  $t = 6552$  hours of tests leads to swelling of the coating due to the sorption of an aggressive medium, which leads to cracking of the protective coating (Fig. 3, a). At the same time, cells with coating peeling were found on the sample's surfaces. These are the end surfaces of the samples, where the thickness of the coating is smaller, and, therefore, the probability of penetration to the base of the aggressive environment is greater. In this way, the adhesive strength of the protective coating with the substrate decreases due to the course of electrochemical oxidation reactions, which leads to edge corrosion.

**Table 2** – The corrosion resistance of epoxy composite coatings after exposure to an aggressive environment of river water for  $t = 6552$  h at temperatures  $T = 258 \dots 303 \pm 2$  K.

Aggressive environment	Change of sample mass, g				
	Epoxy matrix	CM 1	CM 2	CM 3	CM 4
Before exposure, g					
River water (without T-shape cut)	94.3	93.8	96.0	93.2	95.2
	After exposure, g				
	96.1	95.3	97.6	94.1	96.2
	$\chi$ – corrosive resistance, %				
	1.90	1.59	1.66	0.96	1.05
	Coating thickness, $\mu\text{m}$				
	770	780	773	718	727
Before exposure, g					
River water (with T-shape cut)	91,3	91,7	92,1	92,7	92,2
	After exposure, g				
	93.1	93.2	93.7	93.7	93.2
	$\chi$ – corrosive resistance, %				
	1.97	1.63	1.73	1.07	1.08
	Coating thickness, $\mu\text{m}$				
	815	800	805	738	797

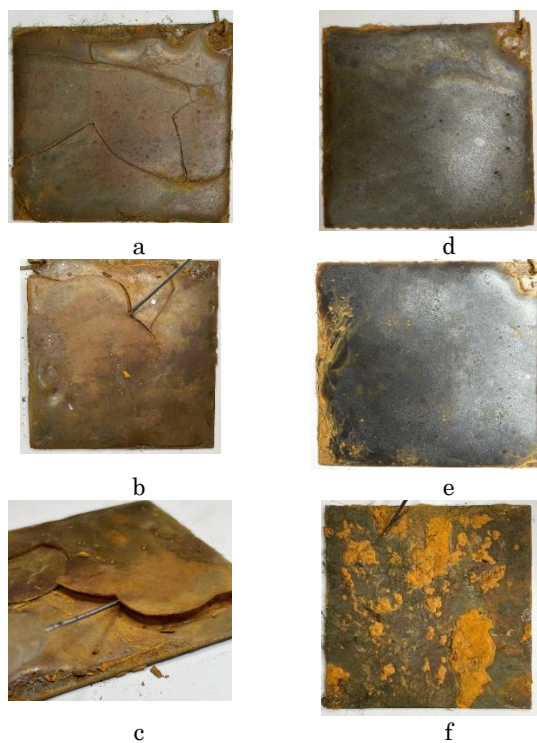


**Fig. 3** – Photos of the applied coating after exposure in river water during  $t = 6552$  hours with temperature range  $T = 258 \dots 303 \pm 2$  K: a – epoxy matrix; b – CM 1; c – CM 2; d – CM 3; e – CM 4; f – metal base without coating (rear side).

For the coating CM 1 cracking defects were observed (Fig. 3, b). At the same time, the value of the permeability index is smaller (compared with the ma-

trix) and is  $\chi = 1.59$  % (Table 2). This is due to the thickness of the protective coating ( $\delta = 780 \mu\text{m}$ ), which is greater than the thickness of the matrix, as well as the change in the structure of the coating with a filler of vegetable origin.

Then, as for the coating CM 2, the value of the permeability index is greater (compared with CM 1) and is  $\chi = 1.66$  %, with the presence of overall peeling of the coating surface (Fig. 3, c), which indirectly indicates on insufficient values of adhesive strength, as well as possible structural defects in the form of micropores, which creates conditions for capillary penetration of an aggressive medium to the base and the formation of a wedging effect (the second Rebinder effect).

Coatings CM 3 and CM 4 demonstrated the absence of defects on their surfaces (Fig. 3, d, e). Accordingly, such coatings are characterized by the smallest values of the permeability index  $\chi = 0.96 \dots 1.05$  % despite the smaller thickness of the coatings –  $\delta = 718 \dots 727 \mu\text{m}$  (Table 2), which indicates the forming of an active barrier to the penetration of aggressive ions and water molecules to the base.

It was supposed that the integrity of the surface of the coating (without defects) is related to the combination of nano-dispersed and fibrous fillers, which ensures the compaction of the spatial polymer grid due to the increase in the number of C-H bonds (confirmed by the method of IR-spectral analysis,  $\nu = 2962 \text{ cm}^{-1}$ ). This means that the optimum content of additives of vegetable origin, on the one hand, ensures a high degree of cross-linking of polymer coatings, and increases hydrophobicity, which in turn prevents the penetration of an aggressive environment, further wedging and the spread of a network of cracks in the structure and on the surface of the coating. On the other hand, the increase of the content of polar functional  $-\text{OH}-$  groups in macromolecules ( $\nu = 3439 \text{ cm}^{-1}$ ) ensures the formation of strong adhesive bonds with the base, which prevents the formation of under-film corrosion and, as a result, the formation of microcracks inside the coating. However, the possibility of the formation of ionic bonds at the boundary of the phase separation "epoxy coating – metal oxide film" was not excluded. If the system "adhesive–substrate" is considered the adhesive is a non-metal and the substrate is a metal. This means that there is a certain negative electric charge with ionic adhesive interaction. Therefore, in this case, it is possible to consider the formation of strong adhesive bonds between the adhesive and the substrate - as a phenomenon of attraction of ions of differently charged bodies. Thus, increasing the number of covalent and ionic bonds in the structure of the polymer coating, as well as between the polymer and the substrate, provides a synergetic effect of improving the barrier protection against the aggressive environment of metal surfaces.

Additionally, the rear side of the metal base is shown (Fig. 3, e). Visual analysis of the samples made it possible to detect, in addition to the corrosion spots on the major part of the surface partial overgrowth of green algae in the form of long, narrow thread-like cells intertwined with each other. It was supposed that a variety of such algae can be attributed to the green algae of the Spirogyra genus. The presence of similar

algae was detected on the surface of the epoxy matrix in the zones with no coating and a coating with minimal thickness (Fig. 3, a).

T-shaped cuts were made on their surface for differing the operating conditions of the coatings, which allows to speed up the course of physical and chemical processes of corrosion. It was established that the epoxy matrix has the highest value of the permeability index  $\chi = 1.97\%$  among the materials under study. In this case, the value of the permeability index is higher by  $\Delta\chi = 0.07\%$  of the coating matrix permeability without a T-cut notch (Table 2). However, in addition to cracking peeling of the coating was observed at the T-cut (Fig. 4, a). This indicates the accumulation of moisture on the hydrophilic centers of the solid phase, which leads to hydrolytic degradation resulting in the peeling of the coating. In addition, the presence of a small amount of green *Spirogyra* algae on the surface of coatings containing cracks was observed.

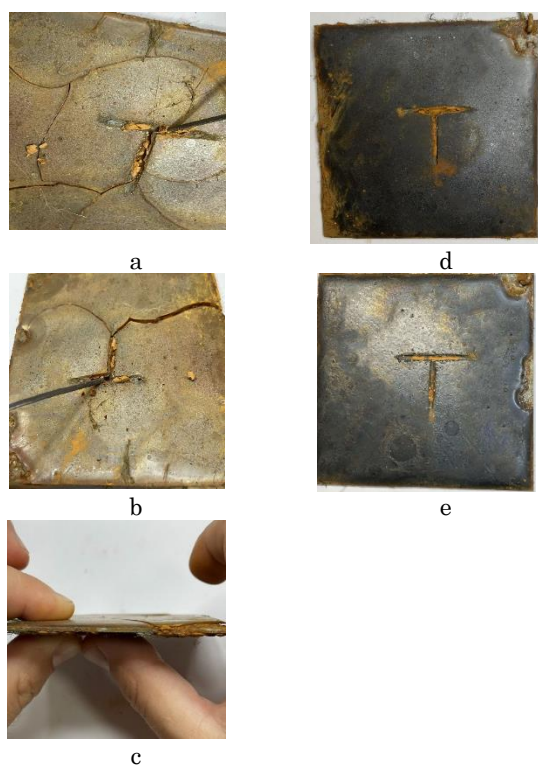


**Fig. 3** – Photos of applied coatings with T-like cuts after exposure in river water for  $t = 6552\text{ h}$  at temperatures  $T = 258 \dots 303 \pm 2\text{ K}$ : a – epoxy matrix; b – CM 1; c – CM 2; d – CM 3; e – CM 4

Similar defects were found for coating CM 1 (Fig. 4, b). However, the value of the permeability index is lower by  $\Delta\chi = 0.34\%$  than for the epoxy matrix (Table 2). In this case, the adhesion strength of the coating containing nanoparticles of vegetable origin to the metal base is higher. Therefore, a decrease in permeability was observed. The resulting defects on the surface of the coating are caused by its structure. That is, the coating does not provide barrier protection of the steel base due to insufficient sealing of the polymer grid. This, in turn, leads to the penetration of an aggressive environment through the smallest thickness of the coating (location of the T-like cut) and ensures

the wedging of the coating in the form of main cracks branching. For the coating CM 2 the value of the permeability index is  $\chi = 1.73\%$ . Visual inspection of the surface (Fig. 4, c) made it possible to establish the delamination of the coating. The obtained image of the coating defect allows us to assert the probable under-film corrosion, which over time led to partial peeling of the protective coating.

Visual inspection of the surface of the coatings CM 3 and CM 4 allows us to determine rather high indicators of corrosion resistance (Fig. 4, d, e). A comparative analysis of the permeability of the aggressive environment of samples with and without a T-shaped cut does not change significantly (Table 2). Based on the comparative characteristics of the corrosion resistance of the developed composite materials in the aggressive environment of river water, it is possible to state that use the following materials to protect the surfaces of parts of the technological equipment of water transport may be considered: CM 3 with the following composition ( $q$ , wt.) – binder: a mixture of discrete fibers based on cotton and polyester ( $l = 15 \dots 30\text{ mm}$ ,  $d = 20 \dots 25\text{ }\mu\text{m}$ ); nanofiller of vegetable origin ( $d = 400 \dots 600\text{ nm}$ ); hardener – 100 : 0.50 : 0.075 : 10; CM 4 with the following composition ( $q$ , wt.) – binder: a mixture of discrete fibers based on cotton and polyester ( $l = 15 \dots 30\text{ mm}$ ,  $d = 20 \dots 25\text{ }\mu\text{m}$ ); nanofiller of vegetable origin ( $d = 400 \dots 600\text{ nm}$ ); hardener – 100 : 0.50 : 0.100 : 10.

#### 4. CONCLUSIONS

1. The degree of crosslinking of the developed composite coatings was investigated using IR spectral analysis. Based on the analysis of changes in the intensity parameters and the relative area of the peaks in the range of wave numbers  $\nu = 400 \dots 4000\text{ cm}^{-1}$ , it was shown that the CM 3 and CM 4 coatings demonstrate resistance to oxidation and other chemical reactions due to the increased degree of cross-linking. This is confirmed by structural changes in epoxy coatings observed at wave numbers:  $\nu = 570\text{ cm}^{-1}$  and  $\nu = 8400\text{ cm}^{-1}$  (an increase of  $-\text{C}-\text{C}-$  bonds),  $\nu = 1045\text{ cm}^{-1}$  (an increase of epoxy groups),  $\nu = 2962\text{ cm}^{-1}$  (an increase of C-H bonds).

2. Series of studies during  $\tau = 6552\text{ hours}$  of exposure in the environment of river water at the temperature of  $T = 258 \dots 303 \pm 2\text{ K}$ , the lowest values of the permeability index were observed for the samples with coatings: CM 3 (thickness –  $\delta = 718 \dots 738\text{ }\mu\text{m}$ ), containing components in the following ratio ( $q$ , wt.) – binder: a mixture of discrete fibers based on cotton and polyester: nanofiller of vegetable origin: hardener – 100 : 0.50 : 0.075 : 10 and CM 4 (thickness –  $\delta = 727 \dots 797\text{ }\mu\text{m}$ ), containing components in the following ratio ( $q$ , wt.) – binder: a mixture of discrete fibers based on cotton and polyester: nanofiller of vegetable origin: hardener – 100 : 0.50 : 0.100 : 10. The developed coatings are characterized by high resistance to penetration of aggressive ions and water molecules into the base (1.8...2.0 times compared to the unfilled matrix) due to high adhesive and cohesive strength, which ensures their long-term operation without surface defects, traces of corrosive destruction and biological fouling products.

## REFERENCES

1. M. Iurzenko, Y. Mamunya, G. Seytre, G. Boiteux, E. Lebedev, *E-Polymers* **11** (2011).
2. K.O. Dyadyura, L.F. Sukhodub, *Proceedings of the 2017 IEEE 7th International Conference on Nanomaterials: Applications and Properties*, NAP 2017, 2017-January, 04NB14 (2017).
3. L. Odnodvoret, S. Protsenko, O. Synashenko, D. Velykodnyi, I. Protsenko, *Crystal Res. Technol.* **44** No 1, 74 (2009).
4. S.I. Protsenko, I.V. Cheshko, D.V. Velykodnyi, L.V. Odnodvoret, I.M. Pazukha, I.Yu. Protsenko, O.V. Synashenko, *Prog. Phys. Metals* **8** No 4, 247 (2007).
5. V. Zaloga, K. Dyadyura, I. Rybalka, I. Pandova, T. Zaborowski, *MSPE* **4**, 28 (2020).
6. V. Zaloga, K. Dyadyura, I. Rybalka, I. Pandova, *MSPE* **4** (2019).
7. G. Hongbo, G. Jiang, H. Qingliang, T. Sruthi, Y. Xingru, H. Yudong, A.C. Henry, W. Suying, G. Zhanhu, *Indu. Eng. Chem. Res.* **52** (2013).
8. R.D. Brooker, A.J. Kinloch, A.C. Taylor, *J. Adhesion* **86** (2010).
9. L. Bilogurova, *Mat.-wiss. u. Werkstofftech* **40**, 4 (2009).
10. M.R. Ayatollahi, E. Alishahi, R. S. Doagou, S. Shadlou, *Compos. Part B: Eng.* **8**, 43 (2012).
11. O.O. Sapronov, A.V. Buketov, P.O. Maruschak, S.V. Panin, M.V. Brailo, S.V. Yakushchenko, A.V. Sapronova, O.V. Leshchenko, A. Menou, *Funct. Mater.* **1**, 26 (2019).
12. P. Valášek, R. D'Amato, M. Müller, A. Ruggiero, *Compos. Part B: Eng.* **146** (2018).
13. M. Milosevic, D. Dzunic, P. Valasek, S. Mitrovic, A. Ruggiero, *J. Compos. Sci.* **7**, 6 (2022).
14. R.A. Kurien, D.P. Selvaraj, M. Sekar, R. Rajasekar, C.P. Koshy, *Mater. Sci. Forum* **1019** (2021).
15. F.Z. Alshammari, K.H. Saleh, B.F. Yousif, A. Alajmi, A. Shalwan, J.G. Alotaibi, *Tribology in Industry* **3**, 40 (2018).
16. N. Barhoumi, A. Ghanem, M. Koudhai, K. Khelifi, Ali Terras Mohamed, *Exp. Polym. Lett.* **5**, 16 (2022).
17. A. Buketov, M. Brailo, S. Yakushchenko, O. Sapronov, V. Vynar, O. Bezbakh, R. Negrutza, *PPME* **3**, 63 (2019).
18. A.V. Buketov, O.M. Sizonenko, D.G. Kruglyj, T.V. Cherniavska, E.S. Appazov, K.M. Klevtsov, Ye.V. Lypian, *Journal of Engineering and Applied Science* **7**, 67 (2020).
19. A.V. Buketov, P.D. Stukhlyak, I.G. Dobrotvor, N.M. Mytnyk, N.A. Dolgov, *Strength of Materials* **4**, 41 (2009).
20. I.H. Dobrotvor, P.D. Stukhlyak, A.V. Buketov, *Mater. Sci.* **6**, 45 (2009).
21. C. Cerbu, *Procedia Technology* **19**, 268 (2015).
22. V. Demchenko, S. Riabov, V. Shtompel, *Nanoscale Res. Lett.* **12** (2017).

### Антикорозійні епоксидні покриття з наночастинками рослинного походження для захисту водних транспортних засобів

О.О. Сапронов<sup>1</sup>, К. Дядюра<sup>2</sup>, П.О. Воробійов<sup>1</sup>, В.Д. Шаранов<sup>3</sup>, М.О. Карпаш<sup>4</sup>, Р.Т. Бішак<sup>5</sup>, Л. Гребеник<sup>6</sup>

<sup>1</sup> Херсонська державна морська академія, пр. Ушакова, 20, 73000, м. Херсон, Україна

<sup>2</sup> Національний університет «Одеська політехніка», 65044, м. Одеса, Одеська область, пр.Шевченка, 1

<sup>3</sup> Дунайський інститут Національного університету «Одеська морська академія», Ізмаїл, Україна

<sup>4</sup> Університет Короля Данила, Івано-Франківськ, Україна

<sup>5</sup> Івано-Франківський національний технічний університет нафти і газу, Івано-Франківськ, Україна

<sup>6</sup> Сумський державний медичний інститут, вул. Троїцька, 28, 40022 Суми, Україна

У статті досліджено структуру розроблених епоксидних покриттів за допомогою ІЧ-спектрального аналізу та корозійну стійкість шляхом визначення індексу проникності в агресивному середовищі річкової води протягом  $t = 6552$  год в діапазоні температур  $T = 258 \dots 303 \pm 2$  К. Показано, що на процес структуроутворення епоксидних покриттів впливає зміна співвідношення нанодисперсних і волокнистих наповнювачів в епоксидному олігомері ЕД-20. Значні структурні зміни для епоксидних покриттів спостерігалися при хвильових числах:  $\nu = 570 \text{ см}^{-1}$ ,  $\nu = 840 \text{ см}^{-1}$ ,  $\nu = 1045 \text{ см}^{-1}$ ,  $\nu = 2962 \text{ см}^{-1}$ , що свідчить про ступінь їх зшивання. Дослідження зміни показника проникності в середовищі річкової води проводили з урахуванням раціонального співвідношення дисперсійних наповнювачів в епоксидному зв'язуючому, що дозволило створити ефективний бар'єр для проникнення агресивних іонів і молекул води до основа. Досягнуто зниження водонепроникності захисних покриттів в 1,8...2,0 рази відносно епоксидної матриці. Крім того, було проведено візуальний аналіз поверхневих покриттів, що експлуатувалися під впливом річкової води при змінних температурах. Для епоксидної матриці та композитів з одним наповнювачем спостерігались дефекти у вигляді тріщин та відшарування, які пов'язані з перебігом фізико-хімічних процесів сорбції та дифузії агресивного середовища. Крім того, для таких покриттів характерна схильність до заростання зеленими водоростями роду *Spirogyra*. Для покриттів, що містять раціональне поєднання двох наповнювачів, спостерігали відсутність дефектів і біологічних забруднень.

**Ключові слова:** Епоксидна Смола, Наповнювач, Аналіз Дефектів, ІЧ-спектральний аналіз, Індекс Проникності, Корозія, Нанопорошок